[Downloaded from www.aece.ro on Thursday, July 03, 2025 at 19:08:59 (UTC) by 172.69.214.215. Redistribution subject to AECE license or copyright.]

High Performance BCD Integrated Buck-Boost Converter in an AMOLED Display with Application of Self-Triggering Frequency Modulation

Hakyun KIM, Seungki JEON, Hoyong CHOI, and Namsoo KIM
School of electrical and computer engineering
Chungbuk National University, Cheong-ju, Chungbuk, 361-763, South Korea
corresponding.nsk@chungbuk.ac.kr

***Abstract*—Feedback control for self-triggering frequency modulation is proposed for an integrated buck-boost DC-DC converter in an AMOLED display. The goal is to reduce the ripple noise and transient time during the switching process. The converter uses two control modes: switching frequency modulation (SFM) mode for light load current and pulse width modulation (PWM) mode for heavy load current, which result in high power efficiency over a wide range of load current. The mode is automatically changed according to the load current and triggering pulse. A ring-type voltage controlled oscillator (VCO) is applied to obtain a proper operating frequency in the feedback control circuit by the load-dependent current source. The set and reset pulses are used to limit the switching-on time in the sensing signals with less transient time. The converter was fabricated with 0.35-μm BCD (BIPOLAR-CMOS-DMOS) process technology. An experiment shows that the maximum power efficiency is 90% over a wide current range of 10 - 150 mA. Compared to a conventional converter, the proposed converter shows significantly less ripple noise and transient time.**

***Index Terms*—DC-DC power converters, CMOS integrated circuits, voltage-controlled oscillators, frequency modulation, pulse width modulation.**

I. INTRODUCTION

Organic light-emitting diode (OLED) displays have advantages in terms of high speed and power efficiency. An active matrix OLED (AMOLED) [1-5] applies the principle of direct light-emission for displays, which allows a significant reduction of the display thickness and weight. The direct light-emission of organic material in AMOLED is significantly dependent on the driving current and voltages which are obtained from the regulator circuit.

An AMOLED display usually requires both negative and positive voltage supplies in the pixel circuit. A dual-mode regulator is conventionally applied to reduce the power consumption and prolong the battery life of a mobile display. The regulator is composed of boost and inverting buck-boost converters. When a mobile phone is in talk mode, the load current is high, and pulse-width modulation (PWM) mode is used to obtain high power efficiency. However, in standby mode, the load current is very low, and pulse-frequency modulation (PFM) mode is usually applied for efficient control.

Generally, there are two types of DC-DC converters that generate a DC source voltage for an AMOLED display [6-9]. One type is based on a single PWM mode. One simple-PWM method uses an inverting buck-boost [6]. It has a simple structure but has the disadvantage of low power efficiency at light load. In a single-inductor multiple-output (SIMO) converter [7], the source voltage of positive voltage V_{POS} is generated by a boost converter, and the source voltage of negative voltage V_{NEG} is generated by the charge pump method. Although the circuit structure is simple, it has a drawback in that maximum power efficiency is low and output ripple voltage is large. Another converter [9] varies the gate voltage of the switching power MOSFET according to the load and has high power efficiency at light load. However, the control circuit is complicated. Since it consists of only the V_{NEG} channel of the inverting buck-boost DC-DC converter, a separate V_{POS} channel converter is required.

The other type of converter is based on dual mode [8]. One dual-mode method combines PWM mode with PSM (pulse skip modulation) mode to increase power efficiency at light load. However, one of its problems is that the output ripple voltage is large due to the random pulse skipping of PSM mode.

This paper proposes a triggering frequency modulation (TFM) control that is composed of SFM and PWM mode. SFM mode operates when there is light load current and PWM is used with heavy load to reduce the ripple noise and obtain high power efficiency during the switching of the load current. In an AMOLED driver circuit, it is challenging to design a high-quality screen with high power efficiency because of the stringent requirement on the output switching ripple and transient response. In this work, frequency modulation is performed by triggering pulses that are obtained from the sensing signals from error amplifier. The set and reset triggering pulses in TFM control provide digitally controlled modulation, and sequential regulation is possible during the pulse interval. Therefore, the power efficiency and regulation accuracy can be improved significantly. Section II discusses the circuit of the PWM-SFM dual-mode inverting buck-boost DC-DC converter. Experimental results are presented in section III, and a conclusion is presented in section IV.

This work was supported by Basic Science Research Program through the National Research Foundation of Korea (NRF) under Grant 2018R1D1A1B07046871 and IDEC.

Digital Object Identifier 10.4316/AECE.2018.03016

1582-7445 © 2018 AECE

[Downloaded from www.aece.ro on Thursday, July 03, 2025 at 19:08:59 (UTC) by 172.69.214.215. Redistribution subject to AECE license or copyright.]

II. Circuit Implementation

The proposed converter uses a voltage-controlled oscillator (VCO) for the frequency control in SFM or PWM mode. In a conventional AMOLED display, an inverting buck-boost converter in the driver circuit requires the DC input voltage to change to a higher or lower negative DC output voltage, depending on the duty ratio of the switching transistor. In this work, the expected output of the converter can be obtained from the change of the switching frequency or duty ratio from the output of the VCO and the reference voltage into the error amplifier.

Fig. 1 shows the structure of the proposed converter, which includes a TFM controller, error amplifier (EA), LC filter, and S-R flip-flop. The TFM controller generates the set and reset switching signals using the VCO and a current sensor that detects the inductor current. The error amplifier [10]-[12] provides its output voltage ER_o to the TFM controller to produce the triggering set (Vs) and reset (V_R) signals. The current sensor also helps to obtain the triggering signals with a proper VCO frequency. Therefore, the selection of PWM or SFM mode is dependent on the sensing current and output ER_o.

The converter runs a current-mode control that keeps the output voltage constant using a feedback control circuit. The control circuit detects the output of the error amplifier and changes the VCO frequency in the PWM/SFM controller to operate in dual modes. With variation of the load current, the converter runs in PWM or SFM mode. PWM mode operates with the change of the duty ratio, and SFM operates with the switching frequency through the TFM controller.

Compared with a conventional dual mode converter, which is composed of PFM and PWM modes, the proposed converter has smaller ripple noise and faster transient time during the switching process. This is possible because the switching-on operation is performed periodically with a limited time interval, which is defined by the set (Vs) and reset (V_R) signals. During this interval, the switching frequency responds to the load and the sensing currents. Pulse skip modulation (PSM) control [8] is similar to the proposed TFM control, but the PSM mode generates an aperiodic signal to obtain a proper regulated switching frequency. PSM mode has an advantage of high power efficiency in the range of light load current, but a random selection of triggering pulses from PSM mode provides a relatively high ripple noise during the on-off switching process. The proposed periodic switching signal has a short time interval that is generated by the set and reset signals. The sequential limited time interval that is supported by the sensing current and feedback control provides faster transient time and smaller ripple noise.

SFM mode is similar to PFM and is used under light load current. The triggering set and reset pulses in SFM mode generate a proper duty ratio and a switching frequency. Fig. 2 shows the simulated waveforms in the PWM-SFM operation. The switching frequency is divided by the critical load current I_{LC}, which is defined by the characteristics of the power efficiency and load current. The figure shows that the set and reset clock signals V_S and V_R provide positive and negative triggering signals in the switching pulse SW.

SFM mode shows an increase of the switching frequency with the load current I_L, while PWM mode has a constant switching frequency with the triggering pulse signals. In the load regulation when the load current changes, PWM mode generates a constant switching frequency with the change of the duty ratio. The duty ratio continues to change until a proper line or load regulation is performed. The transient time and stability of the converter are significantly dependent on the frequency response in terms of the pole-zero locations.

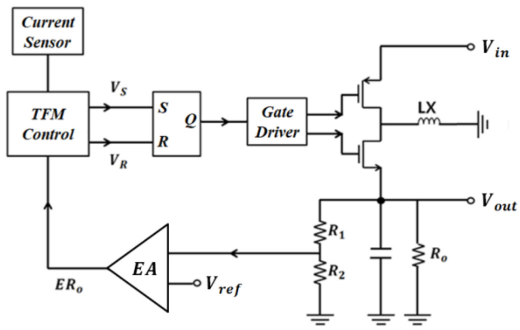

Figure 1. Block diagram of the proposed inverting buck-boost converter with TFM controller

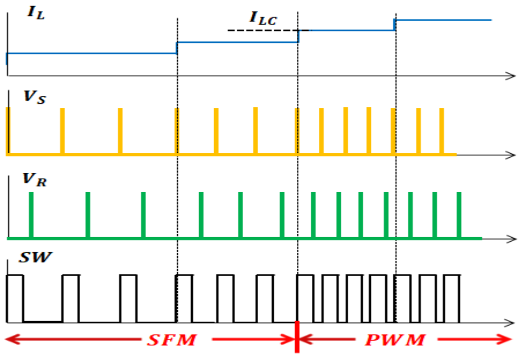

Figure 2. Waveforms in the range of SFM and PWM modes depending on I_{LC}, (a) load current I_L, (b) set clock signal V_S, (c) reset clock signal V_R, and (d) switching pulse SW

Fig. 3 shows a block diagram of the TFM controller. The output voltage ER_o of the error amplifier is one of the inputs of the VCO. The VCO [13-15] generates a sinusoidal signal, which is proportional to the load current. The set signal V_S is obtained from the circuits of the VCO, SR latch, and two comparators. SR latch is used for producing the rising edge pulse and the gate voltage of n-MOSFET which requires for ramp signal. The rising slope of ramp signal is obtained from the capacitor and n-MOSFET. Frequency-dependent signals are obtained from the two comparators which are conventionally used for multi-vibrator circuit or PFM mode controller. The reset clock signal V_R for the operation of the switching-off is obtained from the output current I_E of the error amplifier, ramp signal, and sensing current I_{sense}. The ramp signal is dependent on the load current and frequency. The sensing current comes from the inductor current and is obtained from the aspect ratio between SENSEFET and power FET [16-18].

[Downloaded from www.aece.ro on Thursday, July 03, 2025 at 19:08:59 (UTC) by 172.69.214.215. Redistribution subject to AECE license or copyright.]

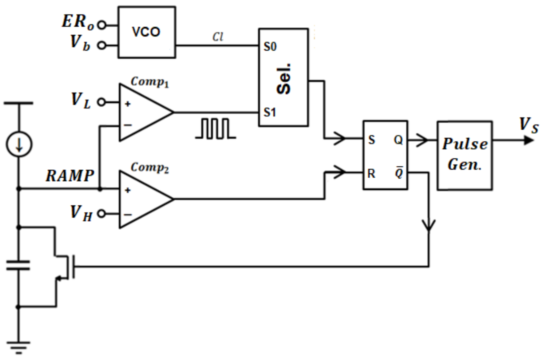

(a)

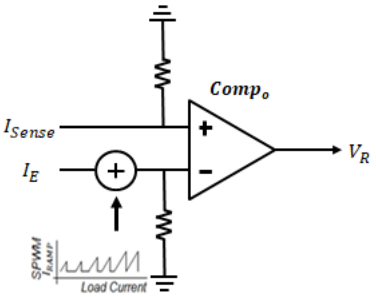

(b)

Figure 3. Block diagram of TFM control circuit for set (a) and reset (b) triggering operations

A block diagram of operation of the TFM controller is shown in Fig. 4. The inputs of the TFM controller are the sensing current I_{sense} and the outputs of the error amplifier I_E and ER_o, which are obtained from the output of the feedback loop. The feedback control continues to change the duty ratio or the switching frequency until an expected output can be obtained. The on-off switching process is done by the power MOSFETs in the power stage of the converter.

A small load current generates a switching pulse of low frequency, which is linearly proportional to the load current. However, when the load current is larger than a critical current (I_{LC}), which depends on the power efficiency, a switching pulse of constant frequency is output, and the variation of the duty ratio provides an expected output that depends on the line and load regulations. In the proposed TFM controller, when the load current reaches the critical current (I_{LC}), the feedback controller changes to PWM mode and works with a constant frequency.

The switching frequency f_{OSC} is determined by equation (1):

$$f_{OSC} = \frac{I_{OSC}}{C_{OSC}\Delta V} \quad (1)$$

where ΔV is the input voltage difference in the error amplifier that generates the bias of the VCO, I_{OSC} is the provided source current, and C_{OSC} is the total combined capacitance in the VCO, which includes the capacitance of the capacitor array. When the load current is light and under the critical current I_{LC} of 30 mA, the switching frequency is designed to operate in the range of 0.1-1.5 MHz. At high load currents above 30 mA, the converter operates with PWM mode, which has a fixed frequency of 1.5 MHz.

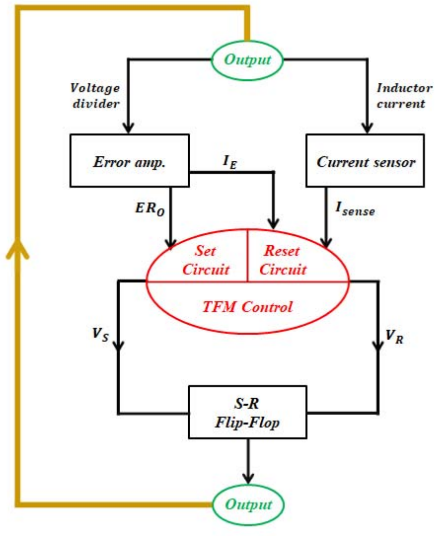

Figure 4. Block diagram of feedback triggering operation with TFM controller

The set and reset signals V_S and V_R provide the positive and negative triggering pulses for the switching pulse (SW), which is important for deciding the duty ratio and the switching frequency. The switching-on process in the power stage of the converter starts from the positive triggering pulse Vs. The triggering pulses pass through the S-R flip-flop, which provides the pulses for PWM and SFM modes.

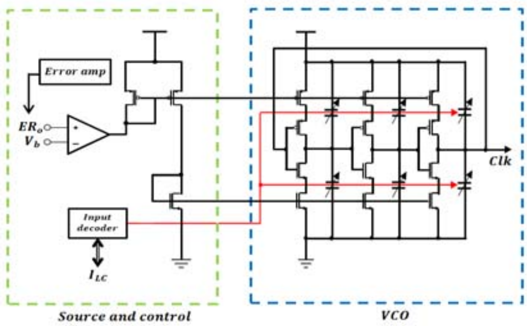

Figure 5. Circuit of the VCO

Fig. 5 shows the circuit of VCO, which includes the structure of a ring oscillator [19-21]. Its simplicity makes it a popular choice in many integrated circuits, such as microprocessors and memories. Three ring-type inverters are used to obtain an oscillating frequency, which depends on the capacitor array and the current source. In the VCO, the current source depends on the output ER_o of the error amplifier, which is also dependent on the feedback stage of the converter. The capacitor array is controlled by an external digital controller and decides the operating frequency based on the combination of capacitors.

III. Experimental Results

The proposed dual-mode buck-boost converter was fabricated with 0.35-μm BCD process technology. Fig. 6 shows a photo of the proposed converter chip, which has an

[Downloaded from www.aece.ro on Thursday, July 03, 2025 at 19:08:59 (UTC) by 172.69.214.215. Redistribution subject to AECE license or copyright.]

area of 4.1 mm^2. Off-chip LC filter is applied with an inductance of 10 µH and capacitance of 10 mF. Experimental work is done with the input voltage of 2.9 - 4.5 V and the switching frequency of 0.1 - 1.5 MHz.

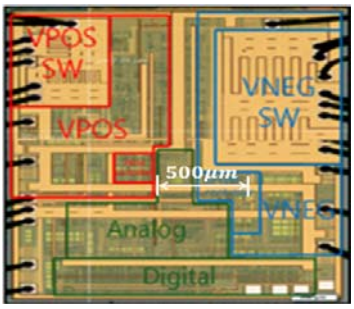

Figure 6. Chip photo

Fig. 7 is a graph which shows the characteristics of VCO output frequency versus the control voltage ER_o, which is the output of error amplifier. 2-bit input decoder is used for the combination of capacitor array and provides a proper critical load current (I_{LC}). The range region of linearity of VCO frequency for the decoder input of [1 1] goes from 0.1 MHz to 1.7 MHz, and the desired output frequency of 1.0 MHz is obtained for a control voltage of 1.26 V.

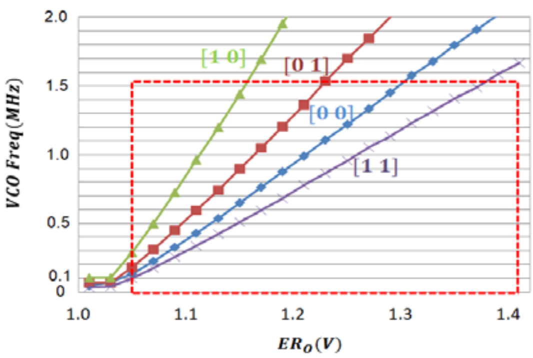

Figure 7. VCO frequency versus control voltage ER_o

Electrical characteristics of the converter, when there are light and heavy load currents, are shown in Fig. 8. In Fig. 8 (a), the output voltage V_{O2} and inductor voltage LX_2 are obtained when the SFM mode operates with light load current of 5 mA, while the result of the PWM operation at the load current of 100 mA is shown in Fig. 8 (b). The results are obtained from the self-triggering operation, which provides the respective switching period of 4 and 0.7 µs in Fig. 8 (a) and (b). The switching frequencies of 0.25 and 1.43 MHz are obtained in SFM and PWM modes. The same outputs of 4.0 V with the ripple voltage of 10 mV are obtained in the two different modes. The small ripple ratio of 0.25 % is a great advantage for the high-quality screen in AMOLED display. The sensing inductor voltage LX_2 in Fig. 8 (b) shows the operation of PWM mode and the approximate duty ratio of 0.5, while that in Fig. 8 (a) shows the high ratio of the off-switching time to prevent the reverse saturating current in the proposed converter. The proposed converter provides the same constant outputs with small ripple ratio at the two different control modes. The switching frequency in SFM mode is supposed to be linearly dependent on the load current I_L, while that in PWM mode is always constant above the critical load current I_{LC}.

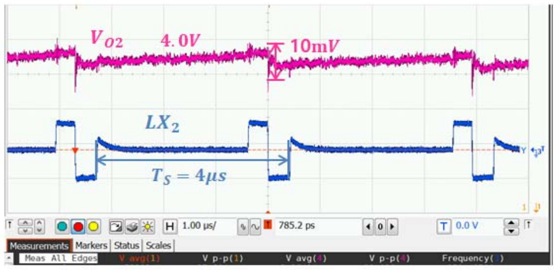

(a) $I_L = 5$ mA

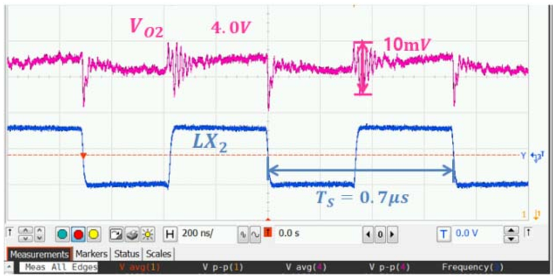

(b) $I_L = 100$ mA

Figure 8. Characteristics of output V_{O2} and inductor voltage LX_2 (a) with SFM mode (5 mA) and (b) PWM mode (100 mA)

The switching characteristics of the proposed and conventional converter are shown in Fig. 9. The comparison shows the transient performance with and without the triggering signal. The output voltage V_{O2} and inductor voltage LX_2 are obtained when the load current I_L changes from null to 60 mA and returns to null. The ripple voltage and switching transient time are important for recent AMOLED displays because they require a high standard of screen brightness and resolution for high-performance displays. When the load current I_L changes from null to 60 mA, the TFM controller is operated with SFM mode under 30 mA and PWM mode above 30 mA of load current. The critical load current I_{LC} is designed to be 30 mA, which depends on the parameters of the VCO and the power efficiency.

The transient time of the proposed converter is reduced to 13.8 µs, which is almost half that of the conventional converter, as shown in Fig. 9 (b). The ripple voltage is also significantly reduced to 21 mV. The reason for the smaller ripple noise and transient time is the triggering pulses that define the switching-on time by sequential pulse generation. The conventional converter usually has non-periodic pulse generation during the abrupt change of load current that occurs in the on-off switching. Longer transient time is required for the output to be stable because there is no restriction on the duration.

[Downloaded from www.aece.ro on Thursday, July 03, 2025 at 19:08:59 (UTC) by 172.69.214.215. Redistribution subject to AECE license or copyright.]

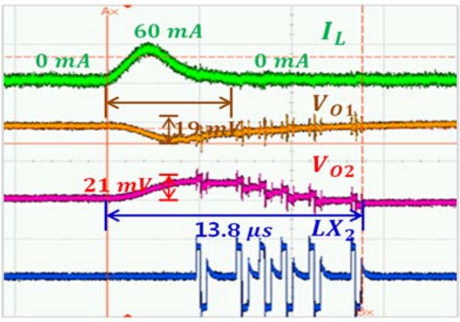

(a)

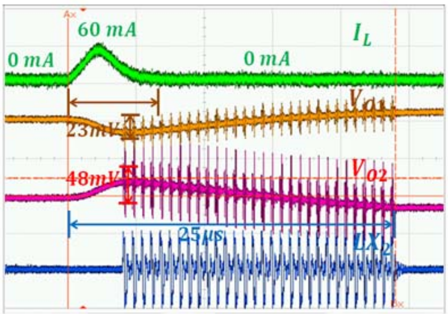

(b)

Figure 9. Switching characteristics of output V_{O2} and inductor voltage LX_2 with change of the load current I_L: (a) proposed converter and (b) conventional converter

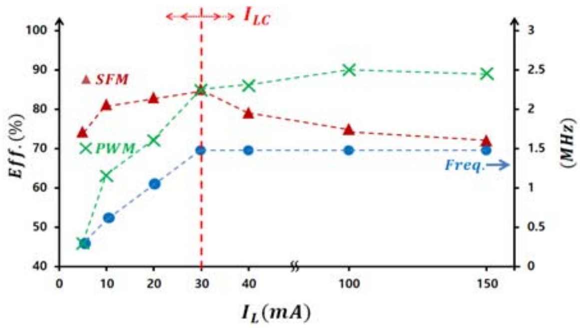

(a)

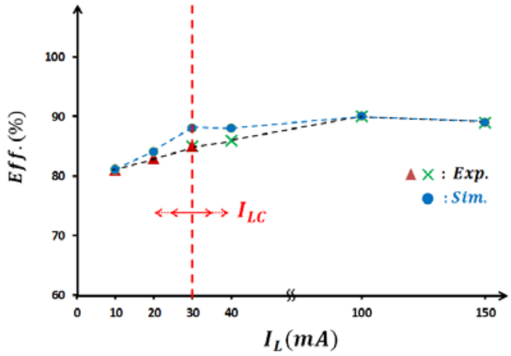

(b)

Figure 10. (a) Power efficiency and operating frequency with change of the load current I_L, (b) Comparison of efficiency between experiment and simulation

The proposed triggering operation is similar to the digital sampling process of an analog signal, which allows only a certain value during a limited time period. The proposed converter with self-triggering pulses is more effective than the conventional one in terms of ripple noise and transient time because the sensing of signals in the feedback circuit are periodically checked by the time-limited triggering pulses.

The power efficiency and frequency were measured with respect to the load current of the converter. In the switching mode converter, the power consumption comes from the on-time resistive loss in the transistors and the switching loss. With light load current, the power loss due to the on-time resistance is more than the switching power loss. The experimental result of the power efficiency and frequency is shown in Fig. 10 (a), which was obtained with a combination of PWM and SFM modes. The operating frequency is also shown with the change of the load current. The PWM mode shows lower power efficiency at load currents under 30 mA, and SFM shows higher power efficiency.

TABLE I. COMPARISON WITH OTHER REPORTED WORKS

		[7]	[9]	[8]	[6]	This work
Year		2009	2015	2012	2014	2017
Mode		PWM	MPLT	PSM-PWM	PWM	SFM-PWM
Technology		0.5μm BiCMOS	0.35μm BCD	N/A	N/A	0.35μm BCD
Chip area [mm^2]		4.1	2.9	N/A	N/A	4.1
Output (V_N)		-5 ~ -8	-4.9	-2.4 ~ -6.4	-1.4 ~ -4.4	-1.4 ~ -5.4
Load current (mA)		~ 240	5 ~ 300	~ 250	~ 250	~ 300
Switching freq. [MHz]		1 (constant)	1 (constant)	1.5 (constant)	1.45 (constant)	0.1 ~ 1.5 (variable)
Ripple [mV] @1mA		N/A	N/A	6.31	N/A	4.02
Trans. time [μs]		N/A	N/A	24	25	13.8
Power effic.	@10mA	57	78	74	74	81
	@200mA	76	83	85	90	88

[Downloaded from www.aece.ro on Thursday, July 03, 2025 at 19:08:59 (UTC) by 172.69.214.215. Redistribution subject to AECE license or copyright.]

Under the critical current, the operating frequency increases linearly with the load current. If the load current exceeds 30 mA, PWM mode is selected with a constant frequency of 1.5 MHz, which is also the maximum frequency of SFM mode. The efficiency at a load current of 10 mA shows an improvement from 63% in PWM mode to 82% in SFM mode. At a load current of 150 mA, the convertor is in PWM mode, and the efficiency is almost 90%. This result indicates that the proposed converter is an efficient high-performance converter that is not affected by the range of output current. Comparison between experimental and simulation results is shown in Fig. 10 (b). Power efficiency from simulation indicates to be higher than that of experiment. In simulation, application of ideal device-parameters in the circuit may increase the efficiency. But, two results show the same characteristic in terms of the dependence of load-current and the range of efficiency.

A comparison summary of DC-DC converter for AMOLED display is presented in Table 1. This work shows the high figure of merit in terms of power efficiency, switching transient time, and ripple noise. High performance is attributed to the self-triggering frequency-dependent pulses and the application of SFM-PWM mode control, which can be applied for a wide range of load current.

IV. Conclusion

A high-performance buck-boost DC-DC converter for AMOLED displays was obtained using a self-triggering TFM controller. The TFM controller operates with a dual-mode converter with self-triggering feedback-loop set and reset pulses, which results in lower ripple noise and transient time during the switching process. The major difference between the conventional and the proposed dual mode converter is the method of control. One uses the separate implementation of PWM and PFM modes, while the other uses the unified control which depends on the frequency and the load current. The set and reset signals for the self-triggering frequency modulation are obtained from the feedback-loop amplifier and sensing circuit. The VCO is operated in SFM or PWM mode with the change of frequency, which is dependent on the current source and capacitor array of the VCO circuit.

The converter was fabricated with 0.35-μm standard BCD process technology, and the chip area is 4.1 mm^2. We obtained high power efficiency of 80 - 90 % for load currents of 20 - 150 mA. The converter operates in SFM mode when under the critical load current of 30 mA and PWM mode when the current is higher. In comparison with a conventional dual-mode converter, the proposed converter shows a significant reduction of ripple noise and transient time during the switching process.

References

[1] B. H. Lee and Y. J. Kim, “ESC-DVS: Dynamic voltage scaling using entropy-based scene change detection for AMOLED displays,” IEEE J. of Elec. Device Soc., vol. 5, pp. 193-208, 2017. doi:10.1109/JEDS.2017.2671426

[2] K. Oh, S. Yang, J. Lee, K. Park, and M. Y. Sung, “Poly-Si TFTs with bottom-gate structure using excimer laser crystallisation for AMOLED displays,” Electronics Letters, vol. 51, issue 24, pp. 2030-2032, 2015. doi: 10.1049/el.2015.2422

[3] Y. H. Fung and Y. H. Chan, “Shaping the spatial and temporal noise characteristics of driving signals for driving AMOLED display,” J. of Display Tec., vol. 12, pp. 1652-1663, 2016. doi: 10.1109/JDT.2016.2618607

[4] H. Ma, Z. Liu, S. Heo, J. Lee, K. Na, H. B. Jin, S. Jung, K. Park, J. J. Kim, and F. Bien, “On-display transparant half-diamond pattern capacitive fingerprint sensor compatible with AMOLED display,” IEEE Sensors Journal, vol. 16, no. 22, pp. 8124-8131, 2016. doi:10.1109/JSEN.2016.2605125

[5] C. Lin, P. Lai, P. Chen, and W. Wu, “Pixel circuit with parallel driving scheme for compensating luminance variation based on a-IGZO TFT for AMOLED display,” J. of Display Tec., vol. 12, pp. 1681-1687, 2016. doi: 10.1109/JDT.2016.2616507

[6] Texas Instruments: “TPS65631: Dual-output AMOLED display power supply,” 2014.

[7] C. S. Chae, H. P. Le, K. C. Lee, and G. H. Cho, “A single-inductor step-up DC-DC switching converter with bipolar outputs for active matrix OLED mobile display panels,” IEEE J. of Solid-State Circuits, vol. 44, no. 2, pp. 509–524, 2009. doi: 10.1109/JSSC.2008.201098

[8] STmicronics: “SOD13AS: Dual DC-DC converter for powering AMOLED display,” 2012.

[9] Sung-Wan Hong, Sang-hui Park, Tae-Hwang Kong, and Gyu-Hyeong Cho, "Inverting buck-boost DC-DC converter for mobile AMOLED display using real-time self-tuned minimum power-loss tracking (MPLT) Scheme with Lossless Soft-Switching for Discontinuous Conduction Mode," IEEE J. of Solid-state Circuits, vol. 50, pp. 2380–2393, 2015. doi: 10.1109/JSSC.2015.2450713

[10] Marn-Go Kim, “Error amplifier design of peak current controlled (PCC) buck LED driver,” IEEE Trans. Power Electronics, vol. 29, no. 12, pp. 6789-6795, 2014. doi: 10.1109/TPEL.2014.2304739

[11] H. Du, X. Lai, C. Liu, and Y. Chi, “Low quiescent current linear regulator using combination structure of bandgap and error amplifier,” Electronics letters, vol. 50, pp. 771-773, 2014. doi: 10.1049/ el.2013.4277

[12] P. Liu, T. Chen, and S. Hsu, “Area-efficient error amplifier with current-boosting module for fast-transient buck converters,” IET Power Electronics, vol. 9, issue. 10, pp. 2147-2153, 2016. doi: 10.1049/ iet-pel.2015.0322

[13] J. Yin, P. Mak, F. Maloberti, and R. Martins, “A time-interleaved ring-VCO with reduced 1/f3 phase noise corner, extended tuning range and inherent divided output,” IEEE J. of Solid-state Circuits, vol. 51, pp. 2979–2991, 2016. doi: 10.1109/JSSC.2016.2597847

[14] Z. Chen, M. Wang, J. Chen, W. Liang, P. Yan, J. Zhai, and W. Hong, “Linear CMOS LC-VCO based on triple-coupled inductors and its application to 40-GHz phase-locked loop,” IEEE Trans. Mic. Theory and Tech., vol. 65, pp. 2977-2989, 2017. doi: 10.1109/TMTT.2017.2663401

[15] S. Ikeda, S. Yeop, H. Ito, N. Ishihara, and K. Masu, “A 0.5 V 5.96-GHz PLL with amplitude-regulated current-reuse VCO,” IEEE Microwave and Wireless Components Letters, vol. 27, issue 3, pp. 302-304, 2017. doi: 10.1109/LMWC.2017.2662001

[16] S. Lee, Y. J. Oh, K. Y. Na, Y. S. Kim, and N. S. Kim, “Integrated BiCMOS control circuits for high-performance DC-DC boost converter,” IEEE Trans. Power Electronics, vol. 28, no. 5, pp. 2596-2603, May 2013. doi: 10.1109/TPEL.2012.2217156

[17] J. M. Liu, P. Wang, and T. Kuo, “A current-mode DC-DC buck converter with efficiency-optimized frequency control and reconfigurable compensation,” IEEE Trans. Power Electronics, vol. 27, no. 2, pp. 869-880, 2012. doi: 10.1109/TPEL.2011.2162079

[18] C. Restrepo, J. Calvente, A. Romero, E. Vidal-Idiarte, and R. Giral, “Current-mode control of a coupled-inductor buck-boost DC-DC switching converter,” IEEE Trans. Power Electronics, vol. 27, no. 5, pp. 2536-2549, 2012. doi: 10.1109/TPEL.2011.2172226

[19] J. Kim, S. Kim, I. Lee, S. Han, and S. Lee, “A low-noise four-stage voltage-controlled ring oscillator in deep-submicrometer CMOS technology,” IEEE Trans. Circuits and Systems-II, vol. 60, no. 2, pp. 71-75, 2013. doi: 10.1109/TCSII.2012.2235734

[20] R. Tao and M. Berroth, “Low power 10 GHz ring VCO using source capacitively coupled current amplifier in 0.12 μm CMOS technology,” Electronics letters, vol. 40, no. 23, pp. 1484-1486, 2004. doi: 10.1049/el:20046514

[21] H. Kim, S. Ahn, and N. Kim, “CMOS integrated time-mode temperature sensor for self-refresh control in DRAM memory cell,” IEEE Sensors Journal, vol. 16, no. 17, pp. 6687-6693, 2016. doi:10.1109/JSEN.2016.2585820